

Hybrid Complementarity Formulations for Robotics Applications

Kishor D. Bhalerao^{1*}, Cory Crean¹, and Kurt Anderson¹

¹ Mechanical, Nuclear and Aerospace Engineering, Rensselaer Polytechnic Institute, USA.

Received XXXX, revised XXXX, accepted XXXX

Published online XXXX

Key words complementarity methods, recursive dynamics, intermittent contact.

MSC (2000) 04A25

The focus of this paper is to review hybrid *recursive-complementarity* formulations for multibody systems characterized by a large number of bilateral constraints which are frequently encountered in robotics. Here, hybrid implies the use of complementarity contact models with recursive forward dynamics schemes. Such formulations have a common underlying structure which can be applied to multibody systems with a constrained tree-type topology. These common steps are pointed out. Theoretical formulation is given for systems using three important classes ($O(n^3)$, $O(n)$ and $O(\log(n))$) of multibody algorithms. Further, numerical comparison for the efficiency is given for rigid multibody systems. The paper makes recommendations on the choice of hybrid complementarity formulations which would result in the most efficient simulation. The paper further gives a non-iterative approach to allow the use of explicit higher order integrators for frictionless contacts. The difficulties in extending this approach to allow for frictional contact are also discussed.

Copyright line will be provided by the publisher

1 Introduction

Modeling intermittent contact for systems characterized by a large number of bilateral constraints is an important problem especially in areas such as robotics and gait analysis. There are two important classes of contact models. The first class involves modeling the deformation at the point of contact while the other focuses on kinematic and impulsive changes in the state [5, 30, 35, 37, 47]. The complementarity contact models fall in the later class and are of primary interest in this paper.

A significant body of literature already exists on describing complementarity contact models and their applications in multibody simulations, a representative of which can be found in [3, 5, 6, 23, 32, 36, 38–40, 40, 45, 47]. The majority of this literature is devoted to modeling contact for rigid multibody systems. [7, 13, 14] describe the contact modeling for deformable bodies using a complementarity approach. The deformation in each body is modeled as a superposition of appropriate mode shape functions. However, the majority of these methods are not optimal for systems characterized by a large number of bilateral constraints.

In this paper, the keyword *hybrid* implies a combination of complementarity contact models with recursive forward dynamics algorithms. The resulting hybrid formulation, unsurprisingly, derives the benefits of the underlying forward dynamics algorithm and the complementarity contact model. Some of the existing hybrid formulations are combinations of complementarity contact models with the *Assembly-Disassembly-Algorithm* [48, 49], *Articulated-Body-Algorithm* [18, 28] and *Divide-and-Conquer Algorithm* [7, 9, 16, 17]. Indeed, there are several other efficient forward dynamics algorithms to simulate rigid and flexible multibody systems some of which can be found in [11, 12, 25–27, 33, 42]. A comparison of the efficiency of some of these schemes is given in [43, 50].

No matter what method one uses, there are certain common steps which one must follow to implement the complementarity contact models resulting in a hybrid scheme. In this paper, these common steps are pointed out. This allows the combination of the complementarity contact models with any recursive forward dynamics method. This paper gives the theoretical development of the hybrid formulation for three important classes ($O(n^3)$, $O(n)$ and $O(\log(n))$) of forward dynamics algorithms, where n denotes the number of generalized coordinates associated with bilateral constraints in the system. The efficiency of the three methods is compared numerically for rigid multibody systems. The paper further makes recommendations for the choice of hybrid formulations which would result in the most efficient simulation. Additionally, the paper also describes a non-iterative explicit higher order integration approach to simulate intermittent frictionless contact.

* Corresponding author, e-mail: kishor8dm@gmail.com, Phone: +01 518 207 7808

2 Underlying mathematical structure

Before proceeding to the hybrid-recursive formulation, the contact model for bodies with no bilateral constraints is discussed. Further, the common steps in formulating the contact constraints are pointed out.

A linear complementarity problem (LCP) can be defined as follows. Given $m \times m$ matrix A and $m \times 1$ vector B , find a $m \times 1$ vector $x \geq 0$ such that $Ax + B \geq 0$ and $x^T(Ax + B) = 0$. The goal is to formulate the contact constraint as an LCP.

2.1 Contact model

The complementarity model consists of a set of conditions which enforce the contact constraints. The intermittent contact models discussed here are described in [3, 45] and briefly included here for the sake of completeness.

Figure 1 shows two bodies which are separated. The least distance between the two bodies is denoted by g_N and is measured between points P and Q . Indeed, for most 3D objects, computing points at least distance itself could potentially be a numerically intensive problem. Some of the possible approaches useful in finding points at least distance can be found in [39] and chapter 2 of [31]. For the current purposes, it is assumed that the points at least distance are directly available from existing software libraries.

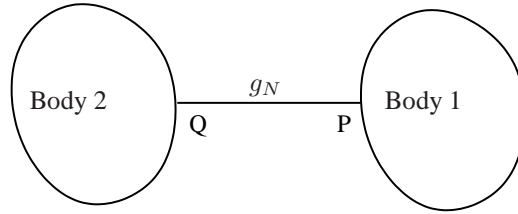


Fig. 1 Proximal points between two convex bodies

If λ_N denotes the contact force acting on each body at the point of contact, then the non-penetration constraint can simply be stated as $0 \leq g_N^{l+1} \perp \lambda_N^{l+1} \geq 0$, where the superscript l denotes the current time. For intermittent contact, it is necessary to impose the non-penetration constraint at position level. The non-penetration constraint can be expressed at velocity level for the case of a continual contact with $g_N = 0$. Another possibility is that of expressing the non-penetration constraint at acceleration level provided that the conditions $g_N = 0$ and $\dot{g}_N = 0$ are satisfied. The strongest condition of the three is the complementarity relationship expressed on position level, since physically the non-penetration constraint is expressed as $g_N \geq 0$ and is of primary interest for the rest of this paper. The other contact constraint is to ensure that the frictional force is dissipative and with a maximum magnitude of $\mu\lambda_N$, where μ denotes the coefficient of friction. In order to avoid a non-linear complementarity problem, a linear approximation of the friction cone is used which results in the frictional force taking the form

$$\mathcal{F} = \{\lambda_N \mathbf{n} + \mathbf{D}_c \boldsymbol{\lambda}_F \mid \lambda_N \geq 0, \boldsymbol{\lambda}_F \geq 0, \mathbf{e}^T \boldsymbol{\lambda}_F \leq \mu \lambda_N\}, \quad (1)$$

where \mathbf{D}_c is a matrix whose columns consist of η unit vectors positively spanning the possible directions of frictional force at the point of contact. \mathbf{n} is the normal at the point of contact, $\mathbf{e} = [1, 1, \dots, 1]^T \in \mathbb{R}^\eta$ and $\boldsymbol{\lambda}_F \in \mathbb{R}^\eta$. Then, the complementarity conditions describing the contact constraint can be written as

$$0 \leq g_N^{l+1} \perp \lambda_N^{l+1} \geq 0, \quad (2a)$$

$$0 \leq \mathcal{S}^{l+1} \mathbf{e} + \mathbf{D}_c^T \mathbf{v}_r^{l+1} \perp \boldsymbol{\lambda}_F^{l+1} \geq 0, \quad (2b)$$

$$0 \leq \mu \lambda_N^{l+1} - \mathbf{e}^T \boldsymbol{\lambda}_F^{l+1} \perp \mathcal{S}^{l+1} \geq 0. \quad (2c)$$

In equation (2), \mathcal{S} is an approximation of the relative tangential contact speed and \mathbf{v}_r is the relative contact velocity vector. Equation (2b) sets the direction of the frictional force while equation (2c) ensures that the magnitude of the frictional force does not exceed $\mu\lambda_N$. In equation (2a), the expression for g_N^{l+1} is obtained via a first order discretization of the velocity equation and can be written as

$$g_N^{l+1} = g_N^l + h \mathbf{n} \cdot \mathbf{v}_r^{l+1} + \epsilon, \quad (3)$$

where h is the time step for the scheme and ϵ is the error introduced due to discretization.

The complementarity conditions in equation (2) describe an inelastic contact. It is straightforward to include restitution based models by incorporating new complementarity conditions after the first impact. The overall process is divided into two phases. In the first phase, sufficient impulse is applied at the point of contact so that $g_N = 0$. During the next time-step, a modified set of complementarity conditions is used depending upon the restitution condition. It is possible to use velocity or impulse restitution in both normal and tangential directions. Details of such restitution models can be found in [2, 3, 24]. The procedure to include these additional complementarity conditions into the recursive scheme is identical to that of the inelastic model. Henceforth, the discussion is limited to the hybrid formulations using an inelastic complementarity model with the understanding that restitution models can be easily incorporated in the same framework.

Using equation (3), equation (2) can be rewritten as

$$0 \leq g_N^l + h \mathbf{n} \cdot \mathbf{v}_r^{l+1} \perp \lambda_N^{l+1} \geq 0, \quad (4a)$$

$$0 \leq \mathcal{S}^{l+1} \mathbf{e} + \mathbf{D}_c^T \mathbf{v}_r^{l+1} \perp \lambda_F^{l+1} \geq 0, \quad (4b)$$

$$0 \leq \mu \lambda_N^{l+1} - \mathbf{e}^T \lambda_F^{l+1} \perp \mathcal{S}^{l+1} \geq 0. \quad (4c)$$

Thus, the complementarity conditions given by equation (4) are to be solved along with the equations of motion for the body to obtain the contact forces. If there are multiple contacts on the body, then each contact is given an identical treatment. A larger LCP must be solved at each time step with the size of the unknown vector dependent on the number of contacts.

2.2 Kinematics and dynamics of a rigid body

Let O denote the origin of a body with an impending contact at point P . If ω and v_P denote the angular and linear velocity of point P , respectively, then the expression for spatial velocity ($\mathcal{V}_P = [\omega \ v^P]^T$) of point P can be written as

$$\mathcal{V}_P = (\mathcal{S}^{rP})^T \mathcal{V}_O, \quad (5a)$$

$$\mathcal{S}^{rP} = \begin{bmatrix} \mathcal{U} & r_P \times \\ \mathcal{Z} & \mathcal{U} \end{bmatrix}_{(6 \times 6)}. \quad (5b)$$

In equation (5), $r_P \times$ is the skew symmetric matrix for realizing the cross product of the matrix representation of the position vector r_P . Vector r_P locates point P with respect to the origin of the body. \mathcal{Z} and \mathcal{U} denote the 3×3 zero and identity matrix, respectively. Similarly, if α and a^P represent the angular and linear acceleration of point P , respectively, then the expression for the spatial acceleration of point P ($\mathcal{A}_P = [\alpha, \ a^P]^T$) can be written as

$$\mathcal{A}_P = (\mathcal{S}^{rP})^T \mathcal{A}_O + \hat{\mathcal{A}}_P, \quad (6a)$$

$$\hat{\mathcal{A}}_P = \begin{bmatrix} 0_{3 \times 1} \\ \omega^O \times (\omega^O \times r_P) \end{bmatrix}_{6 \times 1}. \quad (6b)$$

Next, the equations of motion for this rigid body can be written as

$$\mathcal{M}_O \mathcal{A}_O = \gamma_1 + \gamma_2 \lambda_N + \gamma_3 \lambda_F, \quad (7)$$

where, γ_i are known from the state of the system. \mathcal{M}_O is the spatial mass matrix of the body about the origin O . With this background discussion, the common structure for hybrid recursive formulations is next discussed.

2.3 Common structure for hybrid complementarity formulations

It is clear from the equation (4) that an expression for \mathbf{v}_r^{l+1} is needed as a function of the unknown contact forces to set up an LCP. Here, a useful fact is that the acceleration of any point on the multibody system can always be represented as a linear function of an applied force acting on any point of the system. This statement is true for both rigid and flexible

multibody systems. Noting this fact, the expression for v_r^{l+1} is then obtained via a first order discretization of the expression for acceleration of the point of interest.

For example, consider a body with an impending impact at point P . Assume that the body does not have any bilateral constraints acting on it. Then the expression for the spatial acceleration (\mathcal{A}_O) of the origin ‘‘O’’ can be written as

$$\mathcal{A}_O = \xi_1 + \xi_2 \lambda_N + \xi_3 \lambda_F. \quad (8)$$

In equation (8), the matrices ξ_i are completely known based on the state of the system at time t^l . The next step is to use the kinematic relationship given in equation (6) to obtain an expression for linear acceleration of point P as

$$a_P = \Xi_1 + \Xi_2 \lambda_N + \Xi_3 \lambda_F. \quad (9)$$

The first order discretization of equation (9) gives the expression for the velocity of point P (v_r) as

$$v_p^{l+1} = \tilde{\Xi}_1 + \tilde{\Xi}_2 \lambda_N^{l+1} + \tilde{\Xi}_3 \lambda_F^{l+1}. \quad (10)$$

It should be noted that equation (10) has a first order discretization error. Further, the inverse of the matrix \mathcal{M}_O is embedded in the expressions for $\tilde{\Xi}_i$. This expression can now be substituted in the complementarity conditions given by equation (4) to obtain a linear complementarity problem (LCP) in the form

$$0 \leq \left(\begin{bmatrix} \chi_{11} & \chi_{12} & 0 \\ \chi_{21} & \chi_{22} & \chi_{23} \\ \chi_{31} & \chi_{32} & 0 \end{bmatrix}^l \begin{bmatrix} \lambda_N \\ \lambda_F \\ \mathcal{S} \end{bmatrix}^{l+1} + \begin{bmatrix} \alpha_1 \\ \alpha_2 \\ \alpha_3 \end{bmatrix}^l \right) \perp \begin{bmatrix} \lambda_N \\ \lambda_F \\ \mathcal{S} \end{bmatrix}^{l+1} \geq 0. \quad (11)$$

In equation (11), χ_{ij} and α_i are completely known based on the state vector of the system at time t^l . This is now in the standard LCP form and can be solved using any of the available LCP solvers, e.g. PATH solver described in [19]. The other possibility is to use a scheme based on Gauss-Seidel iterations described in [21]. At this point, it is worth mentioning that the LCP could be side-stepped completely by using a proximal point formulation as described in [21, 29]. However, it has been pointed out in [13] that such alternative formulations are comparable in speed and accuracy to the LCP methods. Henceforth the discussion is limited to formulating and solving an LCP of the form of equation (11). The solution to this LCP gives the contact forces acting over the time-step t^l to t^{l+1} and can be substituted in equation (8) to obtain \mathcal{A}_O . From this expression, a first order Euler integration can be used to obtain the state of the system at time t^{l+1} and the procedure repeats itself.

Thus, the general procedure to formulate the complementarity conditions in the form of equation (11) can be summarized as follows.

- Step 1: As a first step, the expression for the spatial acceleration of the center of mass \mathcal{A}_O (or the origin) of the body is written as a linear function of the unknown contact forces using any appropriate procedure.
- Step 2: Next, using the kinematics of the body, the expression for acceleration of the point of impending contact P is derived. This expression is again a linear function of the unknown contact forces.
- Step 3: A first order discretization of this equation gives the expression for v_r^{l+1} as a linear function of the unknown normal and tangential contact forces. This expression is substituted back into the complementarity conditions given by equation (4) to obtain an LCP in the standard form as given in equation (11).

The procedure described above is unique for a rigid or flexible body which does not have any additional bilateral constraints acting on it. However, for a multibody system with several bilateral constraints, different procedures could be followed to obtain equation (8) resulting in hybrid formulations which are discussed next.

3 Hybrid recursive formulation

The forward dynamics algorithms for rigid multibody systems without algebraic constraints can be broadly classified into three categories, $O(n^3)$, $O(n)$ and $O(\log(n))$, where n denotes the number of generalized coordinates associated with the bilateral constraints in the system. In the following discussion, the development of a hybrid LCP for each of these methods is described.

Irrespective of the chosen forward dynamics method, the three steps described in section 2.3 must be applied for each contact in the multibody system. All forward dynamics methods yield the identical LCP. Consequently, the cost of solving the LCP is identical in each hybrid formulation. Thus, the overall computational cost is governed by the step 1. In the following discussion, it is assumed that there are nb bodies in the system and there is a potential contact on each body.

3.1 Traditional approach

It is possible to write the equations of motion for an unconstrained multibody system in the form

$$M\dot{\mathbf{u}} = \mathbf{F} + \mathcal{G}_N \Lambda_N^{1:nb} + \mathcal{G}_F \Lambda_F^{1:nb}, \quad (12a)$$

$$\implies \dot{\mathbf{u}} = M^{-1}\mathbf{F} + M^{-1}\mathcal{G}_N \Lambda_N^{1:nb} + M^{-1}\mathcal{G}_F \Lambda_F^{1:nb}, \quad (12b)$$

where $\dot{\mathbf{u}}$ denotes the unknown time derivatives of the generalized speeds of the system. The other unknowns in equation (12) are the normal ($\Lambda_N^{1:nb}$) and tangential ($\Lambda_F^{1:nb}$) contact forces. All other terms in equation (12) are known from the state of the system. There are several ways to obtain equation (12) which are collectively referred to as $O(n^3)$ methods.

Equation (12b) is equivalent to the step 1 described in section 2.3. The kinematic relationship described in equation (6) is then used for each body to obtain the expression for acceleration of the point of impending contact in the form $a_P^k = \Xi_1^k + \Xi_2^k \Lambda_N^{1:nb} + \Xi_3^k \Lambda_F^{1:nb}$. Here the superscript k refers to the representative body k in the multibody system. A first order discretization of this equation gives the required expression of \mathbf{v}_r^{l+1} for body k in a form identical to that of equation (10). This expression can now be used in equation (4) for each body to obtain an LCP in the form

$$\mathbf{0} \leq \left(\begin{bmatrix} \chi_{11} & \chi_{12} & \mathbf{0} \\ \chi_{21} & \chi_{22} & \chi_{23} \\ \chi_{31} & \chi_{32} & \mathbf{0} \end{bmatrix}^l \begin{bmatrix} \Lambda_N^{1:nb} \\ \Lambda_F^{1:nb} \\ \mathcal{S}^{1:nb} \end{bmatrix}^{l+1} + \begin{bmatrix} \alpha_1 \\ \alpha_2 \\ \alpha_3 \end{bmatrix}^l \right) \perp \begin{bmatrix} \Lambda_N^{1:nb} \\ \Lambda_F^{1:nb} \\ \mathcal{S}^{1:nb} \end{bmatrix}^{l+1} \geq \mathbf{0}. \quad (13)$$

A significant portion of the literature on the subject (e.g. [2, 3, 40, 45]) follows a procedure similar to the one described above. Such an approach, however, is inefficient for systems characterized by a large number of bilateral constraints which are common in the robotics. This is because there is a $O((n)^3)$ cost involved in formulating equation (12b) from equation (12a). This additional computational cost is avoided on using more efficient forward dynamics algorithms as will be seen in the following discussion.

3.2 Articulated body algorithm (ABA)

There are several $O(n)$ methods for efficient simulation of multibody systems. A majority of these methods follow a common underlying structure which has been described in [25]. A detailed derivation of the ABA for rigid multibody systems is beyond the scope of this paper and the relevant literature is cited in section 1. Here the part relevant to formulating a complementarity problem is discussed.

ABA requires a backward and forward sweep at each time step as shown in figure 2. In absence of contact, the equations of motion for body k during the backward sweep can be written as

$$\mathbf{0} = \mathcal{I}^k \mathcal{A}^k + \mathcal{F}^k, \quad (14a)$$

$$\dot{\mathbf{u}}^k = \tilde{\mathcal{G}}^k \mathcal{A}^k + \tilde{\mathcal{F}}^k. \quad (14b)$$

In equation (14), the unknowns are \mathcal{A}^k and $\dot{\mathbf{u}}^k$. \mathcal{A}^k represents the spatial acceleration of the origin of body k . $\dot{\mathbf{u}}^k$ denotes the time derivative of the generalized speeds associated with the joint between bodies k and $k+1$ as shown in figure 2. The rest of the quantities in equation (14) are known and recursively calculated during the backward sweep.

Next, if it is assumed that each body in the system has a potential impending contact, then equation (14) can be modified as

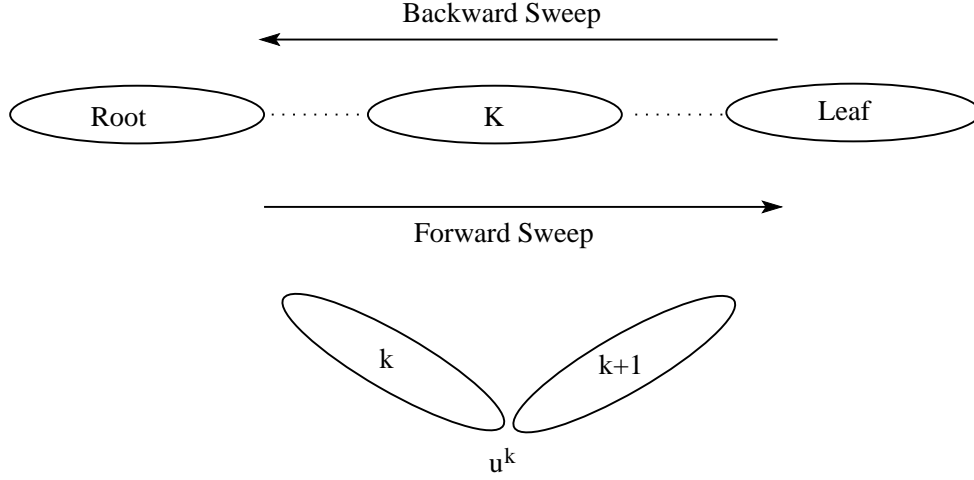


Fig. 2 Articulated Body Algorithm

$$0 = \mathcal{I}^k \mathcal{A}^k + \mathcal{F}^k + \mathcal{G}_N^{k:nb} \Lambda_N^{k:nb} + \mathcal{G}_F^{k:nb} \Lambda_F^{k:nb}, \quad (15a)$$

$$\dot{u}^k = \tilde{\mathcal{G}}^k \mathcal{A}^k + \tilde{\mathcal{F}}^k + \tilde{\mathcal{G}}_N^{k:nb} \Lambda_N^{k:nb} + \tilde{\mathcal{G}}_F^{k:nb} \Lambda_F^{k:nb}. \quad (15b)$$

In equation (15), $\Lambda_N^{k:nb}$ and $\Lambda_F^{k:nb}$ denote the list of normal and tangential contact forces acting on bodies k to nb , respectively. On completing the backward and forward sweep, the expression of the spatial acceleration of origin of each body is obtained as a linear function of the unknown contact forces. This is equivalent to step 1 described in section 2.3. Following the remaining two steps, one obtains an LCP for the system in a form similar to that of equation (13).

For ABA, the procedure one needs to follow to complete step 1 of section 2.3 is identical to that of imposing algebraic constraints on the system at acceleration level at points of impending contact. This is hardly surprising since the goal in both the cases is to obtain the expression of acceleration of appropriate locations as a linear function of an unknown applied constraint force. The primary advantage of using ABA over the more traditional methods is that the cost of this step is linear in the number of joint variables. Indeed, there is an additional cost associated with propagating the unknown contact forces from the body to the root node and back to the body. However, this cost is also linear in the number of intermediate relative joint coordinates encountered. This makes the hybrid ABA-complementarity approach superior to the traditional complementarity approach for multibody system with many bilateral constraints.

3.3 Divide-and-conquer algorithm (DCA)

ABA is optimal for serial implementation but is not well suited for parallel implementation. For several applications (e.g. biped simulation), it is desirable to use parallel algorithms for analysis to achieve increased computational speeds. The DCA presented in [16, 17] achieves a $O(\log_2(n))$ complexity on $O(n)$ processors for tree type topologies. The previous efforts on developing logarithmic complexity algorithms were limited to chain topologies [20] or were iterative [1]. Subsequently, there are other methods (e.g. [11, 34, 49]) which follow the DCA framework with some differences in the actual implementation. A hybrid complementarity formulation is possible with each of these methods. However, here the discussion is limited to the structure of equations for rigid multibody systems with contact. A more detailed description of hybrid DCA-complementarity methods can be found in [7, 9, 48].

DCA consists of two processes, *Assembly* and *Disassembly* which must be carried out at each time step. Figure 3 shows the assembly of two bodies k and $k+1$ of a multibody system. The handle equations for body k can be written following the procedure described in [34] as

$$\mathcal{A}_1^k = \zeta_{11}^k \mathcal{F}_1^k + \zeta_{12}^k \mathcal{F}_2^k + \zeta_{13}^k + \zeta_{14}^k \lambda_N^k + \zeta_{15}^k \lambda_F^k, \quad (16a)$$

$$\mathcal{A}_2^k = \zeta_{21}^k \mathcal{F}_1^k + \zeta_{22}^k \mathcal{F}_2^k + \zeta_{23}^k + \zeta_{24}^k \lambda_N^k + \zeta_{25}^k \lambda_F^k. \quad (16b)$$

In equation (16), \mathcal{F}_1^k and \mathcal{F}_2^k are the spatial constraint forces acting on handles H_1^k and H_2^k , respectively. The handle equations can be written for all the bodies in the system in this form. On performing the *Assembly-Disassembly* operation (see [7, 9] for details), one obtains

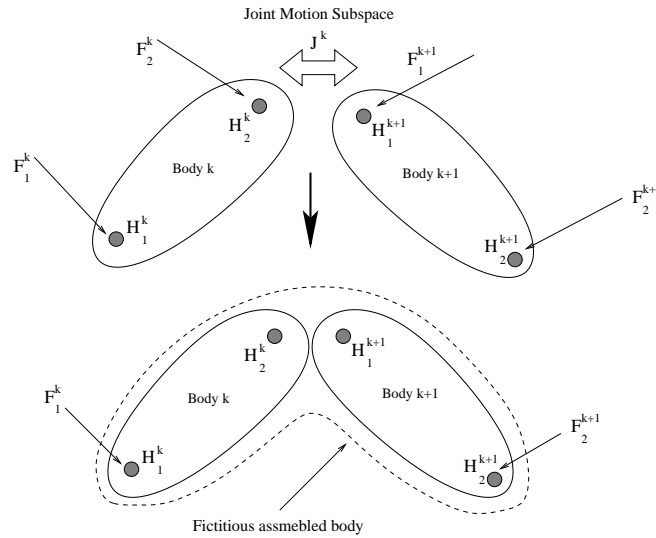


Fig. 3 Divide-and-Conquer Algorithm

$$\mathcal{A}_1^k = \mathcal{G}_{11}^k + \mathcal{G}_{12}^k \Lambda_N^{1:nb} + \mathcal{G}_{13}^k \Lambda_F^{1:nb}, \quad (17a)$$

$$\mathcal{A}_2^k = \mathcal{G}_{21}^k + \mathcal{G}_{22}^k \Lambda_N^{1:nb} + \mathcal{G}_{23}^k \Lambda_F^{1:nb}. \quad (17b)$$

Equation (17) completes step 1 as described in section 2.3. Following the procedure described in steps 2 and 3, it is possible to obtain an LCP for the system in a form identical to that of equation (13). As was the case with ABA, the procedure to obtain the LCP for contact constraints in DCA is same as the procedure which needs to be followed to impose algebraic constraints. Each point of contact is treated as an additional handle and on performing the *Assembly-Disassembly* operation, the expression for spatial acceleration of the point of contact on each body is obtained as a linear combination of the unknown contact forces. Thus, the order of method remains unchanged for formulating the LCP.

3.4 Numerical comparison of hybrid complementarity methods

In the previous section, the procedure for hybrid complementarity methods was given along with the theoretical computational complexity in formulating the LCP. In this section a numerical comparison is given for the three classes of methods. All the methods are serially implemented. The system consists of an nb rigid body planar chain which is released from rest under the influence of gravity as shown in figure 4. All the bodies in the system are initially held in a horizontal position at a height of 1 above the ground and are identical with mass and length equal to 1. Each simulation is performed for the duration of 2 seconds with a fixed time step of 10^{-3} . The number of bodies selected for timings studies are 1,2,4,8,16,32,64 and 128.

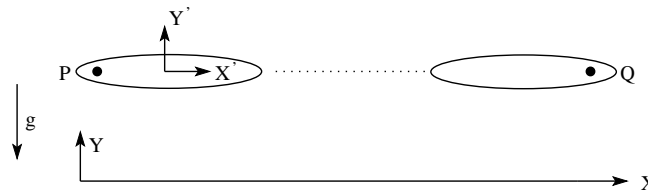


Fig. 4 System simulated for time comparison

Figure 5 shows the timing comparison for the three methods in absence of any contacts. The simulations are performed in Matlab and the average time taken for 5 runs are reported in figure 5. The plot of efficiency of the methods was as expected. Although DCA and ABA are both $O(n)$ methods for serial implementation, DCA is slower than ABA due to the excess matrix manipulations required as compared to ABA.

Next, the efficiency of each method is tested in presence of contacts. Two different cases are simulated. An inelastic contact is defined, first between point P and line $y = 0$ and then between points P and Q and the line $y = 0$. Figure 6 gives the comparison of the efficiency of the hybrid complementarity methods. The plots can be explained as follows.

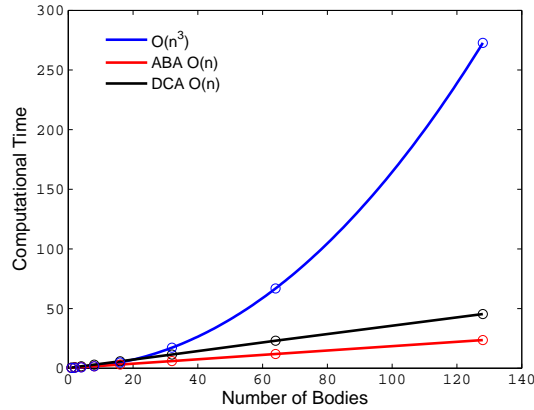


Fig. 5 Computational efficiency of three different methods in absence of contact

In each hybrid method, the three steps discussed in section 2.3 are followed. The computational cost of steps 2 and 3 are comparable in all hybrid formulations. Consequently, the overall cost of the hybrid methods is dictated by step 1. The additional computational cost of solving the LCP is identical in all hybrid formulations.

The overall cost of the traditional method is, unsurprisingly, $O(n^3)$ as is clearly seen in figure 6(a). The vertical shift in the efficiency curve in presence of contacts corresponds to the additional time required to solve the LCP.

In DCA and ABA, the efficiency curves shown in figures 6(b) and 6(c) for no contact and one contact are exactly parallel. This was also anticipated and can be explained as follows. The point P is chosen as the root node in both the methods. Consequently, the unknown contact forces appear in the equation only on reaching the root node. At this point an LCP can be set up and solved to obtain the contact forces. Thus, the backward and forward sweeps (*assembly* and *disassembly* for DCA) are identical with one contact and with no contacts. However, the situation is different in presence of two contacts. In that case, the unknown contact forces from point Q are propagated back to the root node. At this stage, the expression for the acceleration of point P can be obtained as a linear function of unknown contact forces at points P and Q . This however, is not sufficient to set up an LCP. Consequently, the forward sweep must be completed to obtain an expression for acceleration of point Q as a linear function of the unknown contact forces at points P and Q . At this point an LCP can be set up in the usual manner and solved for to obtain the contact forces. The additional cost of propagating the unknown contact force from point Q to the root node and back is also $O(n)$ in both DCA and ABA for serial implementation. This additional cost is reflected in the change in slopes of the efficiency curves for two contacts in both DCA (figure 6(b)) and ABA (figure 6(c)). Figure 6(d) gives a comparison of all the three hybrid methods in presence of two contacts.

These results can now be extrapolated to the more general case of an nb body chain with an arbitrary number of contacts. The efficiency of hybrid complementarity methods is primarily dictated by step 1 of section 2.3. In each hybrid formulation, the cost of formulating an LCP for each additional contact is comparable. As a result, the choice of forward dynamics algorithm for efficiently formulating an LCP is independent of the number of potential contacts in the system. This implies that if a forward dynamics algorithm for a given system topology is most efficient in absence of any contact, the same method would also be the best in presence of an arbitrary number of contacts. The results from existing literature for the efficiency of forward dynamics algorithms are briefly summarized here.

For serial implementation with $n > 7$, the $O(n)$ method is faster than the traditional $O(n^3)$ approach [43]. The order of an $O(n)$ method is the same for a chain and branched topology for unconstrained systems. However, an $O(n)$ method incurs an additional $O(nm^2 + m^3)$ cost associated with m independent algebraic constraints. A better approach for such constrained systems is to use *Recursive-Coordinate-Reduction* (RCR) [10] which results in an $O(n + m)$ formulation.

For parallel implementation, a DCAe-complementarity [11] approach would achieve the fastest results when used for larger systems. Other parallel algorithms such as DCA [16, 17], ADA [49] and ODCA [34] are also expected to achieve an improved performance over traditional methods when used with the complementarity contact models. However, the obtainable speedups for branched topologies are highly dependent on the structure of the *assembly* tree. A more detailed discussion on the subject can be found in section 2 of [17]. A comparison of some of the parallel forward dynamics algorithms is given in [50].

Based on the above discussion, a suitable method for an efficient simulation may be selected depending upon the system under consideration and the computational architecture available.

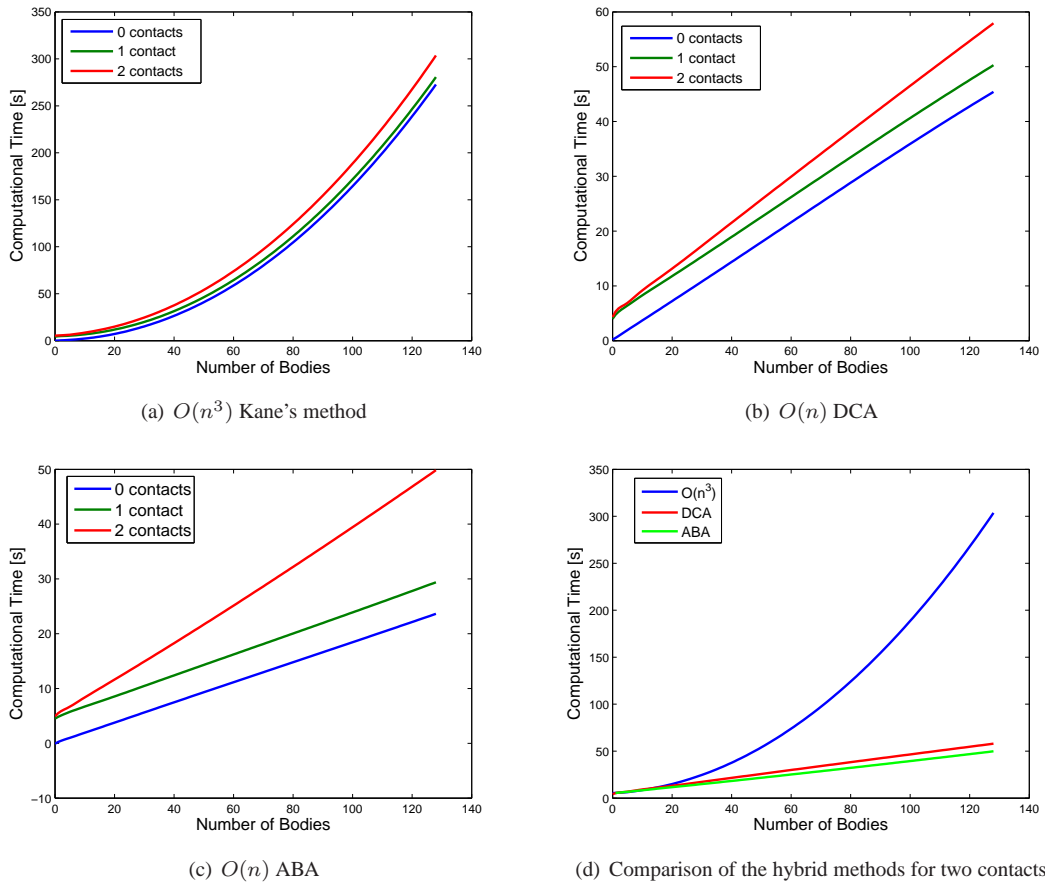


Fig. 6 Computational efficiency of the hybrid complementarity methods

4 Accuracy of Complementarity Time-Steppers

It is possible to formulate an LCP following the procedure described in section 2.3, solution to which yields the contact forces. In this section, the accuracy of the complementarity based time-steppers is discussed along with several practical issues pertinent to simulation of multibody systems frequently encountered in robotics.

Recall that the complementarity formulation is dependent on the first order discretization of the acceleration equation of the point of contact. Here it is worth mentioning that the contact force and acceleration are theoretically infinite and cannot be calculated at the exact time of impact. However, the way around this was to look at the impulse ($I_c = \int_{\delta t} F_c dt$) instead of the contact force F_c at each contact. In all the complementarity time-stepping schemes, the contact impulse is approximated using a first order discretization as $I_c \approx \Delta t F_c$, where $\Delta t = t^{l+1} - t^l$ is the fixed time-step of integration. This allows the expression of acceleration, also referred to as ‘pseudo-acceleration’ in [29], to be written as described before. The set of contact forces obtained from solving the LCP are such that the contact constraints are satisfied as long as a first order Euler integration is employed for the integration of the equations of motion. However, a first order integration is rarely used in any multibody simulation.

A higher order method for simulating frictional contact problems is given in [44, 46]. This approach assumes some information about the nature of solution and the discontinuities resulting from the *stick-slip* phenomenon in presence of friction. [29] describes a four-stage Runge-Kutta method for contact problems which achieves fourth order accuracy during the smooth parts of the motion and a first-order accuracy if an impact is encountered during the time-step. These methods are still inadequate for several important systems which encounter an impact at every time-step, e.g. bipeds and tracked vehicles. An iterative higher order integration scheme for deformable bodies undergoing intermittent contact is described in [13, 15]. The derivation is given for both explicit and implicit higher order integration. This approach requires that g_N be expressed as a linear function of the generalized coordinates. To achieve this, absolute coordinates are used to describe the position and orientation of each body and a Taylor series expansion is employed. This, however, is rarely possible for 3D systems employing internal coordinates. A second order method for frictional contact which requires the solution of

a single LCP per time step is described in [22, 41]. This method does not make any restrictive assumption to achieve the second order convergence and hence differs from those cited before.

In the following discussion, a non-iterative scheme for frictionless contact is described which allows the use of any explicit higher order integration method along with the complementarity solver. The difficulties in extending this method to include frictional contacts are also discussed.

4.1 Explicit Higher Order Integration for Frictionless Contact

As stated before, although the contact forces are infinite, their effect is approximated ($I_c = \Delta t F_c$) in the time-stepping scheme using a first order discretization. This practice is common for all complementarity time-steppers and the solution to the LCP yields the contact impulse I_c . The contact impulse is further used to compute the state of the system at time t^{l+1} without computing the acceleration. However, the state of the system at time t^{l+1} can also be computed by assuming that a constant force $F_c = \frac{I_c}{\Delta t}$ acts on the system from time t^l - t^{l+1} as long as a first order integration is used to integrate the equations of motion. This idea is further extended to allow for any higher order explicit integration scheme as follows.

First, calculate the contact impulses (I_c) acting over the time-step Δt using the standard LCP procedure. Next, equivalent constant contact forces F_c are computed using $F_c = \frac{I_c}{\Delta t}$. At this point the state of the system is known at time t^l . All the forces acting on the system are known for the time-step t^l - t^{l+1} . As a result, any higher order integration scheme can be utilized to integrate the system from time t^l to t^{l+1} . This simple modification however has some other numerical effects on the contact problem. The first and most obvious problem is that the complementarity conditions given in equation (4) are no longer exactly satisfied. The complementarity conditions would be satisfied only if a first order Euler integration was used to advance the simulation. Indeed, on using a first order integration, the complementarity conditions can be satisfied to a user defined precision. However, the resulting simulation would be of little practical use because of the large errors present in the system as a consequence of using a first order integration for a highly non-linear system.

To demonstrate this point, a simple 8 planar body pendulum as shown in figure 4 is simulated using a forward Euler integration and a Runge-Kutta 4th order integration with a fixed time step of 10^{-3} s. There are no contacts defined in the system and the point P is connected to ground via revolute joint. The system is released from a horizontal position with zero initial velocity and allowed to move under the influence of gravity. The system is expected to conserve energy since there are no dissipative forces acting on it. As can be clearly seen from figure 7, the first order integration introduces errors of magnitude $O(10^6)$ higher than the explicit Runge-Kutta integration. This result easily shows that even if the complementarity conditions are exactly satisfied to a high degree of precision, the first order Euler integration introduces significant errors in the simulation. This is especially true for highly non-linear systems frequently encountered in robotics.

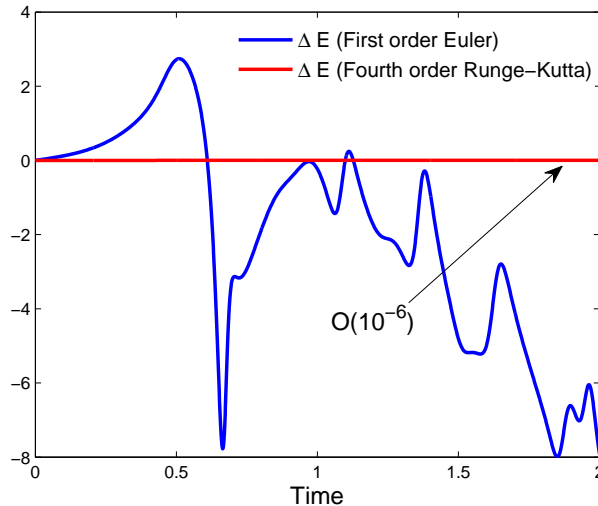


Fig. 7 Drift in total energy, $\Delta t = 10^{-3}$ s.

Thus, in the modified higher order time-stepper, some errors are certainly introduced in satisfying the complementarity conditions. It is numerically demonstrated that such errors are still of an acceptable magnitude. The system shown in figure 4 is simulated for 3 bodies with a frictionless inelastic contact defined between points P, Q and line $y = 0$. In the initial state, the center of mass of the first body is located at point $(x, y) = (0, 2.3)$ and its orientation angle with respect

to ground fixed reference frame is $-\frac{\pi}{6}$. The other relative angles are set to 0. Since the chosen system does not have any frictional force acting on it, it is expected that the center of mass of the system should not change in the x direction. Further the complementarity conditions should enforce a non-penetration constraint at points P and Q . The results are shown in figure 8 and the drift in center of mass in x direction is denoted by δ_{CM} .

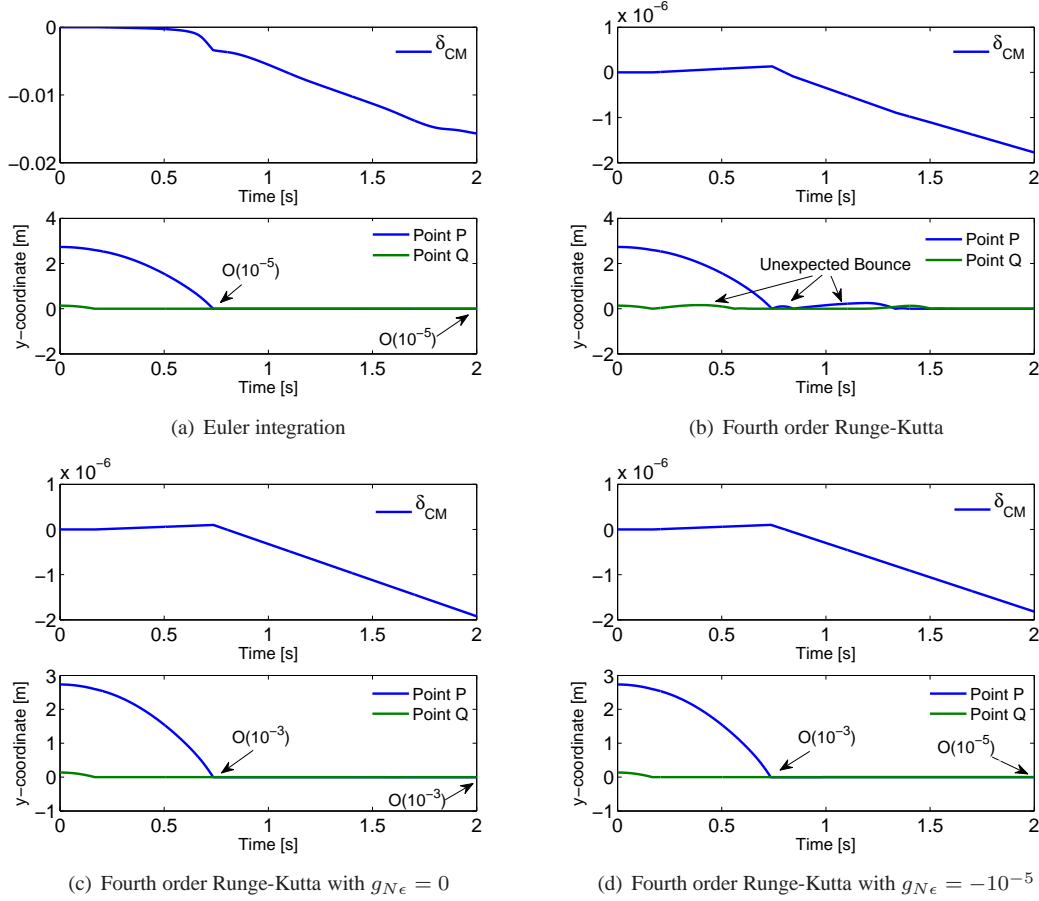


Fig. 8 Accuracy of complementarity time-steppers. $\Delta t = 10^{-3}$, $\mu = 0$.

Figure 8(a) shows that a first order integration causes a significant drift in the center of mass of the system. This drift is magnified by an order of magnitude for a 3D system as has been shown in [9]. The error in inter-penetration constraint is of $O(10^{-5})$ which is acceptable.

Next, an explicit fourth order Runge-Kutta integrator is employed following the procedure described in the beginning of this section and the results are shown in figure 8(b). The drift in the center of mass is improved by a factor of $O(10^4)$ as compared to the Euler integration. However, an unexpected bounce is encountered at the points of inelastic contact. This can be explained as follows. The forces obtained from the LCP are such that the complementarity conditions are satisfied if a first order integration is used. However, in this case the forces obtained from the LCP solver are used in a fourth order Runge-Kutta integration. This violates the non-penetration constraint ($g_N^{l+1} < 0$) to a much higher degree than the case with forward Euler integration ($g_N^{l+1} \approx 0$). If the contact occurred between time $t^l - t^{l+1}$, then the system is under considerable strain at time t^{l+1} as $g_N^{l+1} < 0$ and $|\dot{g}_N^{l+1}| > 0$. If the non-penetration constraint is again imposed at the position level, the simulation gives incorrect contact forces for the time-step $t^{l+1} - t^{l+2}$. This is because the contact force applied between $t^{l+1} - t^{l+2}$ is, by definition, sufficient to reverse the direction of motion of the point of contact so that $g_N \approx 0$ at time t^{l+2} based on a first order discretization. This results in physically incorrect and excessively large forces being applied on the system during the time-step $t^{l+1} - t^{l+2}$.

This problem, however, can be easily resolved by switching the position level complementarity constraint to a velocity level constraint after the first impact. The new complementarity condition is then simply stated as $0 \leq \mathbf{n} \cdot \mathbf{v}_r^{l+2} \perp \lambda_N^{l+2} \geq 0$. Indeed, the actual implementation of this modified condition is trivial and can be achieved by the following simple conditional statement in the simulation code. If ($g_N^l < 0$), then set $g_N^l = 0$. This automatically ensures that once contact is established, the position level non-penetration relationship is replaced by complementarity condition at velocity level. The

additional advantage is that as soon as the contact is lost, the complementarity condition automatically changes to position level. Figure 8(c), shows that on switching the complementarity constraint to velocity level on impact, the bounce seen previously (see figure 8(b)) disappears. However, the inter-penetration constraint errors are two orders of magnitude higher than those seen in figure 8(a). Another possible drawback of such an approach is the accumulation of position level errors as the simulation progresses [8].

This problem can be corrected in the following manner. Previously, the complementarity solver was not allowed to see any inter-penetration by imposing the complementarity condition at velocity level after the first impact. In order to correct this, the amount of inter-penetration seen by the complementarity solver is limited explicitly with another small modification to the conditional statement. If $(g_N < g_{N\epsilon})$, then set $g_N = g_{N\epsilon}$, where $g_{N\epsilon} \leq 0$ is user defined and is dependent on the time-step of integration and the system chosen. The effect of this modification is that the contact force applied by the complementarity solver is not exceedingly large. However, care must be taken in selecting the value of $g_{N\epsilon}$ since setting $g_{N\epsilon} < 0$ for a certain time-step is equivalent to adding a small amount of energy to the system during this time step to correct the errors in inter-penetration constraint. Indeed, the value of $g_{N\epsilon}$ is not arbitrary and it is possible to make an intelligent guess. The value of $g_{N\epsilon}$ is of the same order as the errors in inter-penetration constraint introduced on using a first order integration. In this case, the forward Euler integration results in an inter-penetration error of the order of $O(10^{-5})$. Hence, $g_{N\epsilon} = -10^{-5}$. With this modification, the errors introduced in the inter-penetration constraint on the first impact are reduced by two orders of magnitude as seen from figure 8(d). This clearly shows that the errors introduced in the complementarity condition due to use of the higher order integration can be kept in control. At the same time, the accuracy of the overall simulation is improved by four orders of magnitude.

Using a higher order integration following the procedure described above has some important disadvantages for frictional contacts. The frictional force is no longer guaranteed to be dissipative or achieve maximum dissipation. In the traditional LCP approach, it is possible to prove that the frictional force obtained on solving the LCP achieves maximum dissipation as long as a first order integration is employed to advanced the simulation. However, it must be pointed out that the maximum dissipation is limited by the number of directions of friction associated with the polygonal approximation of the friction cone (the columns of matrix \mathcal{D}_c is equation (1)) chosen at each contact. In other words, it is possible to get closer to the theoretical maximum dissipation by selecting a sufficiently large number of direction vectors. This is not done in practice. Additionally, the first order integration required to prove the maximum dissipation itself cannot be treated as a truth model due to the large errors introduced in the integration of equations of motion.

The proposed approach is expected to work well for frictionless contacts. In the presence of friction, the method is not guaranteed to produce accurate results.

4.2 Practical Issues with Flexible Multibody Systems

The hybrid formulations described above can directly be extended to include flexible bodies in the systems as well and have been described in [7, 13–15]. A *Floating Frame of Reference* approach is employed to model the deformation in each body. All the discussion regarding the accuracy of integrators is directly applicable for flexible bodies as well. Modeling contact in flexible bodies gives rise to additional difficulties which are briefly discussed in this section.

The steps given in section 2.3 can be used for a hybrid complementarity formulation for flexible multibody systems. The deformation field in each body is modeled as a superposition of preselected mode shape functions. During the impact of a flexible body, all the possible deformation modes of the body are excited. It is not physically possible to include all the mode shapes in the simulation. In the least, the mode shapes which are expected to play an important role in restitution of the flexible body must be included. Here it should be noted that the simulation can be performed without including the higher order modes. This however does not guarantee an accurate simulation. The errors introduced in the simulation on neglecting the higher order mode shapes excited on impact are expected to depend on the system under consideration and its effects are hard to quantify. Note that a velocity or impulse restitution model can also be included for flexible bodies. However, in reality, the elastic behavior of the body is responsible for the restitution. Consequently, the high frequency modes which do not play a significant role in the dynamics of the system in absence of contact must also be included for a correct contact simulation.

This leads to other problems. The error introduced in the expression for v_r^{l+1} (see equation (10)) now also depends on the frequency of the mode shapes. Consequently, the accuracy of the computed contact forces depends on the frequency of the mode shape and the time steps of integration. Including high frequency mode shapes would then demand smaller time-steps to control the errors in the simulation. For such systems it is better to use the complementarity contact models described in [4, 41] to account for the stiffness of each flexible body.

5 Conclusion

This paper discussed the simulation of intermittent contact in robotic systems characterized by a large number of bilateral constraints. A clear guideline is given for hybrid complementarity formulations which allows the use of complementarity contact models with any of the recursive forward dynamics schemes. Each hybrid formulation results in an identical LCP. The cost of solving this LCP is the same in all the hybrid formulations. Consequently, if a forward dynamics algorithm is optimal for a given system in absence of any contact, the same algorithm would also be optimal in presence of contacts. Thus, the comparative studies of recursive forward dynamics schemes for serial [43] and parallel implementation [11, 50] directly apply to the case of simulating multiple contacts using a hybrid LCP formulation. Additionally, it was theoretically and numerically shown that the traditional approach for including complementarity contact models in multibody systems with many bilateral constraints is inefficient. The traditional approach for modeling intermittent contact is expected to give optimal results for smaller systems. A hybrid $O(n)$ -complementarity method results in the most efficient implementation for larger systems simulated on a single processor. In presence of parallel architecture, any of the $\log(n)$ -complementarity methods would result in an efficient simulation.

Additionally, a modified approach for integration of motions is presented which allows the use of any explicit higher order integrator with the LCP solver for frictionless contact. For frictionless case, it is numerically demonstrated that such a modified approach is better than the first order integration required for the traditional LCP time-steppers. In the presence of friction, this modified approach could result in inaccurate simulations. Using higher order integrators for intermittent frictional contact results in well documented difficulties and is not possible without making some restrictive assumptions about the system. Currently, the only method to achieve a second order convergence is described in [22, 41] and should be the method of choice for simulating intermittent frictional contact.

References

- [1] K. S. Anderson and S. Duan, A hybrid parallelizable low order algorithm for dynamics of multi-rigid-body systems: Part I, Chain systems, *Mathematical and Computer Modeling* **30**, 193–215 (1999).
- [2] M. Anitescu, A fixed time-step approach for multi-body dynamics with contact and friction, Tech. Rep. ANL/MCS-P1034-0303, Mathematics and Computer Science Division, Argonne National Laboratory, Argonne, Illinois, 2003.
- [3] M. Anitescu and F. Potra, Formulating multi-rigid-body contact problems with friction as solvable linear complementarity problems, *ASME Journal of Nonlinear Dynamics* **14**, 231–247 (1997).
- [4] M. Anitescu and F. Potra, A time-stepping method for stiff multibody dynamics with contact and friction, *International Journal for Numerical Methods in Engineering* **55**(7), 753–784 (2002).
- [5] A. A. Barhorst, On modelling variable structure dynamics of hybrid parameter multibody systems, *Journal of Sound and Vibration* **209**(4), 571–592 (1998).
- [6] D. Barhorst, Issues in computing contact forces for non-penetrating rigid bodies, *Algorithmica* **10**, 292–352 (1993).
- [7] K. Bhalerao and K. Anderson, Modeling intermittent contact for flexible multibody systems, *Nonlinear Dynamics* **60**(1-2), 63–79 (2009).
- [8] K. Bhalerao, On Methods for Efficient and Accurate Design and Simulation of Multibody Systems, PhD thesis, Rensselaer Polytechnic Institute, 2010.
- [9] K. D. Bhalerao, K. S. Anderson, and J. C. Trinkle, A recursive hybrid time-stepping scheme for intermittent contact in multi-rigid-body dynamics, *Journal of Computational and Nonlinear Dynamics* **4**(4), 041010 (2009).
- [10] J. H. Critchley and K. S. Anderson, Recursive coordinate reduction method for multibody systems dynamics, *Journal of Multiscale Computational Engineering* **1**(2-3), 181–199 (2003).
- [11] J. H. Critchley, K. S. Anderson, and A. Binani, An efficient multibody divide and conquer algorithm and implementation, *Journal of Computational and Nonlinear Dynamics* **4**(2), 021004 (2009).
- [12] S. Duan and K. S. Anderson, Parallel implementation of a low order algorithm for dynamics of multibody systems on a distributed memory computing system, *Engineering with Computers* **16**(2), 96–108 (2000).
- [13] S. Ebrahimi, A Contribution to Computational Contact Procedures in Flexible Multibody Systems, PhD thesis, University of Stuttgart, 2007.
- [14] S. Ebrahimi and P. Eberhard, On the use of linear complementarity problems for contact of planar flexible bodies, *Proceedings of the ECCOMAS Thematic Conference on Multibody Dynamics* (2005).
- [15] S. Ebrahimi and P. Eberhard, A linear complementarity formulation on position level for frictionless impact of planar deformable bodies, *Zeitschrift fuer angewandte Mathematik und Mechanik* **86**(10), 808–817 (2006).
- [16] R. Featherstone, A divide-and-conquer articulated body algorithm for parallel $O(\log(n))$ calculation of rigid body dynamics. Part 1: Basic algorithm, *International Journal of Robotics Research* **18**(9), 867–875 (1999).
- [17] R. Featherstone, A divide-and-conquer articulated body algorithm for parallel $O(\log(n))$ calculation of rigid body dynamics. Part 2: Trees, loops, and accuracy, *International Journal of Robotics Research* **18**(9), 876–892 (1999).
- [18] R. Featherstone, *Robot Dynamics Algorithms* (Kluwer Academic Publishers, Boston, Massachusetts, 1987).
- [19] M. Ferris and T. Munson, Interfaces to PATH 3.0: Design, implementation and usage, *Computational Optimization and Applications* **12**(1), 207–227 (1999).

- [20] A. Fijany, I. Sharf, and G. M. T. D'Eleuterio, Parallel $O(\log n)$ algorithms for computation of manipulator forward dynamics, *IEEE Transactions on Robotics and Automation* **11**(3), 389–400 (1995).
- [21] M. Foerg, F. Pfeiffer, and H. Ulbrich, Simulation of unilateral constrained systems with many bodies, *Multibody System Dynamics* **14**, 137–154 (2005).
- [22] B. I. Gavrea, M. Anitescu, and F. A. Potra, Convergence of a class of semi-implicit time-stepping schemes for nonsmooth rigid multibody dynamics, *SIAM Journal on Optimization* **19**(2), 969–1001 (2008).
- [23] C. Glocker and F. Pfeiffer, Multiple impacts with friction in multibody systems, *Nonlinear Dynamics* **7**, 471–497 (1995).
- [24] C. Glocker and C. Studer, Formulation and preparation for numerical evaluation of linear complementarity systems in dynamics, *Multibody System Dynamics* **13**(4), 447–463 (2005).
- [25] A. Jain, Unified formulation of dynamics for serial rigid multibody systems, *Journal of Guidance, Control, and Dynamics* **14**(3), 531–542 (1991).
- [26] S. S. Kim and E. J. Haug, Recursive formulation for flexible multibody dynamics: Part I, Open-loop systems, *Computer Methods in Applied Mechanics and Engineering* **71**(3), 293–314 (1988).
- [27] S. Kim and E. Haug, A recursive formulation for flexible multibody dynamics, Part II: closed loop systems, *Computer Methods in Applied Mechanics and Engineering* **74**(3), 269 (1989).
- [28] E. Kokkevis, Practical physics for articulated characters, in: *Proceedings of Game Developers Conference*, (2004).
- [29] R. Leine and C. Glocker, A set-valued force law for spatial Coulomb–Contensou friction, *European Journal of Mechanics/A Solids* **22**(2), 193–216 (2003).
- [30] P. Loetstedt, Mechanical systems of rigid bodies subject to unilateral constraints, *SIAM Journal of Applied Mathematics* **42**(2), 281–296 (1982).
- [31] B. Mirtich, *Impulse-based Dynamic Simulation of Rigid Body Systems*, PhD thesis, University of California at Berkeley, 1996.
- [32] J. J. Moreau, Unilateral contacts and dry friction in finite freedom dynamics **302** (1988).
- [33] R. Mukherjee and K. S. Anderson, A logarithmic complexity divide-and-conquer algorithm for multi-flexible articulated body systems, *Computational and Nonlinear Dynamics* **2**(1), 10–21 (2007).
- [34] R. Mukherjee and K. S. Anderson, An orthogonal complement based divide-and-conquer algorithm for constrained multibody systems, *Nonlinear Dynamics* **48**(1-2), 199–215 (2007).
- [35] M. S. Pereira and P. Nikravesh, Impact dynamics of multibody systems with frictional contact using joint coordinates and canonical equations of motion, *Nonlinear Dynamics* **9**, 53–71 (1996).
- [36] F. Pfeiffer, Applications of unilateral multibody dynamics, *Phil. Trans. R. Soc. Lond.* **359**(1789), 2609–2628 (2001).
- [37] F. Pfeiffer, The idea of complementarity in multibody dynamics, *Archive of Applied Mechanics* **72**(11-12), 807–816 (2003).
- [38] F. Pfeiffer, Unilateral multibody dynamics, *Multiscale Computational Engineering* **1**(2 & 3), 311–326 (2003).
- [39] F. Pfeiffer and C. Glocker, *Multibody Dynamics with Unilateral Contacts*. Wiley Series in Nonlinear Sciences (Wiley, New York, 1996).
- [40] F. Pfeiffer and C. Glocker, *Multibody Dynamics with Unilateral Constraints*, CISM Courses and Lectures No. 421, International Centre for Mechanical Sciences (Springer, 2000).
- [41] F. Potra, M. Anitescu, B. Gavrea, and J. Trinkle, A linearly implicit trapezoidal method for integrating stiff multibody dynamics with contact, joints, and friction, *International Journal for Numerical Methods in Engineering* **66**(7), 1079–1124 (2006).
- [42] S. K. Saha and W. O. Schiehlen, Recursive kinematics and dynamics for parallel structured closed-loop multibody systems, *Mechanical Structures and Machines* **29**(2), 143–175 (2001).
- [43] W. Stelzle, A. Kecskemethy, and M. Hiller, A comparative study of recursive methods, *Archive of Applied Mechanics* **66**(1-2), 9–19 (1995).
- [44] D. Stewart, A high accuracy method for solving odes with discontinuous right-hand side, *Numerische Mathematik* **58**(1), 299–328 (1990).
- [45] D. E. Stewart and J. C. Trinkle, An implicit time-stepping scheme for rigid body dynamics with inelastic collisions and coulomb friction, *International Journal of Numerical Methods in Engineering* **39**, 2673–2691 (1996).
- [46] D. Stewart, A numerical method for friction problems with multiple contacts, *The ANZIAM Journal* **37**(03), 288–308 (2009).
- [47] J. Trinkle, D. Pang, S. Sudarsky, and G. Lo, On dynamic multi-rigid-body contact problems with Coulomb friction, *Zeitschrift für Angewandte Mathematik und Mechanik* **77**(4), 267–279 (1997).
- [48] K. Yamane and Y. Nakamura, A numerically robust LCP solver for simulating articulated rigid bodies in contact, *Proceedings of Robotics: Science and Systems IV, Zurich, Switzerland* (2008).
- [49] K. Yamane and Y. Nakamura, Efficient parallel dynamics computation of human figures **1**, 530–537 (2002).
- [50] K. Yamane and Y. Nakamura, Comparative study on serial and parallel forward dynamics algorithms for kinematic chains, *International Journal of Robotics Research* **28**(5), 622–629 (2009).